Functional Validation of an Implantable Medical Dosing Device by MRI at 3T

Jeff R. Anderson, Silvia Ferrati, Chistof Karmonik, and Alessandro Grattoni

Abstract— **Sustained release of a small molecule from a prototype implantable drug delivery device was monitored via MRI in an ex vivo tissue phantom over a period of two days. T1 mapping was used as a method to quantify analyte concentration. Continuous, controlled release was observed. The MRI methodology was thus found to be appropriate for device validation and quality assurance/control.**

I. Introduction

Sustained administration of medications presents specific advantages over more traditional dosing schedules including less fluctuation in blood drug levels, frequency reduction in dosing, enhanced convenience and compliance, and reduction in adverse side effects [1]. For drugs that require parenteral administration, sustained administration via an implantable device can also have a positive effect on quality-of-life [2]. Novel, implantable medical devices created to this end can have, as design goal, drug release extending over many days making validation of prototype efficacy a challenge.

One approach for device validation is to construct a realistic tissue phantom that can be monitored over time by magnetic resonance imaging (MRI) or some other imaging modality. This paper presents such an approach. An MR-compatible prototype implantable device was constructed and placed within a tissue phantom. Sustained release of a low molecular weight contrast agent was quantified over a period of 48 hours.

II. Methods

A. Tissue Phantom Preparation

An implantable medical device was manufactured from polyether ether ketone (PEEK) and silicon. The device was preloaded with 0.5 M Magnevist (Bayer Healthcare AG, Leverkusen, Germany) and was suspended in 1% agar (w/v) in a container of approximate dimensions 5×5×2 cm in order to simulate implantation into soft tissue in vivo. Magnevist, a commercially available MRI contrast agent, was chosen as its molecular weight approximates that of the intended deliverable.

B. MRI Image Acquisition

All imaging was carried out on a 3T Philips Ingenia MRI (Philips Healthcare, Best, The Netherlands; Magnetic Resonance Imaging facility of the Houston Methodist Research Institute, http://www.houstonmethodist.org/mri-core) with an eight-channel wrist coil (Invivo, Gainesville, FL, USA). The phantom was imaged immediately following setting of the agar (t = 0 hours), at t = 23 hours, and at t = 46 hours.

A fast inversion recovery approach was adopted utilizing a turbo spin echo pulse sequence to image T1 throughout the whole phantom at all time points. Imaging parameters were as follows: TR = 10 s, TE = 7.6 ms, ETL = 10, FOV = 160 x 160 x 128, and res = 0.5 x 0.5 x 1.0 mm with six inversion times (0.10, 0.35, 0.60, 1.25, 2.50, and 4.50 s).

The phantom was also imaged with an ultrashort TE (UTE) pulse sequence in order to visualize the device itself. Imaging parameters were as follows: TR = 13.6 ms, TE = 0.154/2.938 ms, and flip angle = 8 degrees, and FOV = 128 x 128 x 128 with isotropic 0.5 mm resolution. A difference image between the two echo times was used to visualize the implantable device only.

C. Data Analysis

Quantitative T1 maps were fitted from the inversion recovery data using the appropriate three parameter equation [3].

$$S(TI) = A \cdot e^{-TI/T1} + B$$

where S is the signal intensity, TI is inversion time, and A and B are fitted constants influenced by, among others, the bulk magnetization, coil weighting, and flip angle calibration. Magnevist concentration (C) was estimated from the T1 by taking 3.7 $mM^{-1}s^{-1}$ to be the longitudinal relaxivity (r1) of Magnevist in 1% agar [4,5] and 0.48 s^{-1} to be the longitudinal relaxation rate constant (R1) of 1% agar in the absence of Magnevist (R10, measured).

$$R1 = r1 \cdot C + R10$$

Concentration as a function of distance from the exit ports of the implantable device was modeled as a monoexponential decay with a constant offset. The decay constant was estimated at each time point.

III. Results

Contrast agent was observed in the agar gel tissue phantom following implantation of the drug delivery device. At each time point, the concentration of contrast agent was highest near the exit ports of the implantable device and decreased in a radial pattern from that point (Figure 1).

J. R. Anderson and C. Karmonik are with the MR Core Facilites at the Houston Methodist Research Institute, Houston, TX 77030 USA (phone: 713-441-0803; fax: 771-441-0845; e-mail: JRAnderson@houstonmethodist.org and CKarmonik@houstonmethodist.org).

S. Ferrati and A. Grattoni are with the Department of Nanomedicine at the Houston Methodist Research Institute, Houston, TX 77030 USA (e-mail: SFerrati@houstonmethodist.org and AGrattoni@houstonmethodist.org).

978-1-4244-7929-0/14/$26.00 ©2014 IEEE

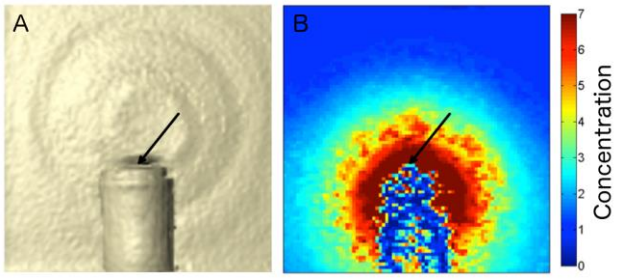

Figure 1. A) Volume rendering of the implantable medical device using the UTE pulse sequence. Note that the ridges seen in the image correspond to real contours on the bottom of the phantom container. B) Concentration map at t = 46 hours. Arrows in both figures highlight the location of the cluster of exit ports of the implantable device.

Concentration maps at each time point are shown in Figure 2. These data reveal that the concentration external the implantable device increased as a function of time, but that the radial pattern of contrast agent distribution was retained.

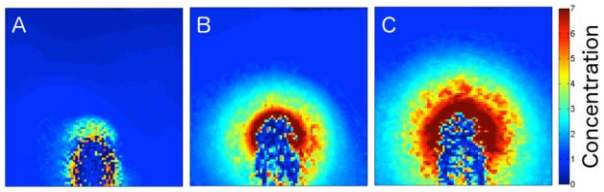

Figure 2. Concentration of contrast agent in the tissue phantom at 0, 23, and 46 hr (Panels A, B, and C, repsectivley).

Concentration as a function of distance from the exit ports of the implantable device is shown in Figure 3. All three time points are displayed along with the modeled decay. The rate constant of concentration as a function of distance was found to be 0.15 with a standard deviation of 0.04 mm^{-1}.

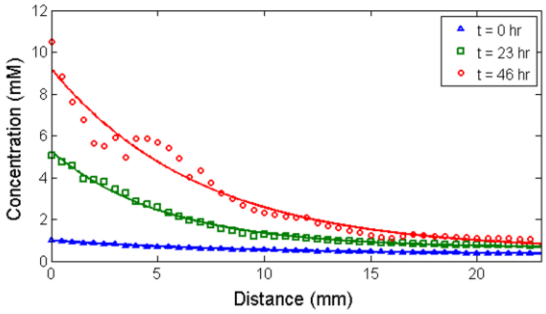

Figure 3. Concentration of contrast agent in the tissue phantom at 0, 23, and 46 hr (Panels A, B, and C, repsectivley).

IV. Discussion

MRI is a noninvasive imaging modality that does not utilize ionizing radiation and has excellent contrast between soft tissues. MR-compatible dosing devices would enable monitoring response to a particular medical dosing schedule via MRI, which, depending upon the application, may be the preferred monitoring method. As is presented in this paper, imaging can also be used as a way to validate dosing devices temporally and spatially.

The radial dispersion of Magnevist observed in Figure 2 validates that the analyte is exiting the implantable device only, as intended, at the exit ports of the device. That is, the device does not appear to demonstrate any unwanted leaks. The dispersion pattern also provides a means to evaluate the spatial delivery pattern of the device. For instance, this geometry could be compared to a second device of similar shape but containing ports at two locations on the device.

The sustained, consistent release over the measured time points indicates that Magnevist is continually being delivered to the agar "tissue" over an extended period of time. The rate of drug delivery can be quantified by the modeled rate constants. This then can be used as a tool for comparing multiple device geometries. For instance, comparisons could be made between devices with similar shapes, but varied numbers of exit ports.

In this first proof of principle experiment, the "tissue" container was relatively small. This limited the measureable timecourse of the experiment as the rate of delivery is expected to slow as the concentrations of contrast agent in the two compartments (external and internal the implanted device) approach parity. However, simply increasing the size of the tissue container can extend the measureable timecourse. Thus, the container appears infinitely large for a longer period of time.

V. Conclusion

This study illustrates the utility of MRI to validate and test the efficacy of implantable medical devices in a agar-based tissue phantom. The current device was found to show precise and sustained infusion of analyte into the gel medium. This promising result has led to further validation in animal models of implantation currently underway.

References

[1] L. V. Allen Jr., N. G. Popovich, and H. C. Ansel, *Ansel's Pharmaceutical Dosage Forms and Drug Delivery Systems*, 9th ed., Baltimore, MD: Lippincott Williams & Wilkins, 2010, ch. 9

[2] C. D. Saudek et al., "Implantable Insulin Pump vs Multiple-Dose Insulin for Non-Insulin-Dependent Diabetes Mellitus," *JAMA: Journal of the American Medical Association*, vol. 276(16), Oct. 1997, pp. 1322-1327.

[3] P. B. Kingsley, "Methods of measuring spin-lattice (T_1) relaxation times: An annotated bibliography," *Concepts in Magnetic Resonance*, vol. 11(4), June 1999.

[4] M. Rohrer, et al., "Comparison of magnetic properties of MRI contrast media solutions at different magnetic field strengths," *Investigative Radiology*, vol. 40(11), pp. 715-724, Nov. 2005.

[5] G. Stanisz and M. Henkelman, "Gd-DTPA relaxivity depends on macromolecular content," *Magnetic Resonance in Medicine*, vol. 44(5), pp. 665-667, Nov. 2000.